Nanofabrication of a two-dimensional array using laser-focused atomic deposition

R. Gupta, J. J. McClelland,[a] Z. J. Jabbour, and R. J. Celotta
Electron Physics Group, National Institute of Standards and Technology, Gaithersburg, Maryland 20899

(Received 16 May 1994; accepted for publication 27 June 1995)

Fabrication of a two-dimensional array of nanometer-scale chromium features on a silicon substrate by laser-focused atomic deposition is described. Features 13 ± 1 nm high and having a full-width at half maximum of 80 ± 10 nm are fabricated in a square array with lattice constant 212.78 nm, determined by the laser wavelength. The array covers an area of approximately $100\ \mu\text{m}\times200\ \mu\text{m}$. Issues associated with laser-focusing of atoms in a two-dimensional standing wave are discussed, and potential applications and improvements of the process are mentioned.

New methods for fabrication of nanometer-scale structures have been under intensive investigation recently because of the perceived benefits which might arise, such as smaller electronic devices, higher-density information storage, and novel materials. Within the past three years, a new technique for nanostructure fabrication involving laser-focused atomic deposition has been demonstrated.[1–3] In this paper we present a significant enhancement of the original technique, which was used to fabricate lines on a substrate, to demonstrate the first two-dimensional fabrication. With these new results, we also discuss some of the considerations associated with generalizing the dimensionality of the process.

In laser-focused atomic deposition, a laser light-field is used to control the motion of atoms as they deposit onto a surface. This approach has a number of potential advantages in comparison with conventional fabrication techniques, such as optical or electron-beam lithography. The advantage over optical lithography lies in the potential for much higher resolution. Optical techniques are fundamentally limited by diffraction to a minimum feature size of about half the wavelength of the light used. For ultraviolet light, this corresponds to about 100 nm. Free-flying thermal atoms, on the other hand, have De Broglie wavelengths of order 10 pm, so diffraction effects can in principle be reduced to a negligible level. The actual resolution limits of laser-focused atomic deposition are still a subject of research, though structures have already been demonstrated at the 65 nm level and theoretical predictions suggest that 5–10 nm features may be possible.[2]

This range of feature size is already just attainable with electron beam lithography;[4] however this process is inherently serial, that is, a complex pattern must be fabricated by scanning the electron beam across the surface. For large, complex patterns, the fabrication time and associated drift problems make electron beam lithography less desirable. Laser-focused atomic deposition, on the other hand, does not suffer from these limitations because it can be implemented in a parallel fashion.

A one-dimensional schematic of the two-dimensional laser-focused atomic deposition process used in the present work is shown in Fig. 1. A laser standing wave is generated across the surface of the substrate, and chromium atoms, collimated to 0.25 mrad in each of two dimensions by laser cooling,[5] are directed at the surface, traversing the laser field on their way to deposition. The laser field, produced by a single-frequency CW dye laser, is tuned 500 MHz (100 natural line widths) above the atomic resonance line in chromium at $\lambda=425.55$ nm (vacuum wavelength). With this tuning, a dipole force[6] is exerted on the atoms toward the low intensity regions of the light field. The result is a concentration of atoms at the nodes of the standing wave, which occur at intervals of $\lambda/2=212.78$ nm.

In one dimension, the process as depicted in Fig. 1 is relatively straightforward. One aspect of the geometry illustrated in Fig. 1 that simplifies the implementation of this process is the fact that the positions of the deposited lines on the substrate depend only on the standing wave node positions, which in turn depend primarily on the absolute distance along the substrate from the mirror generating the standing wave. To first order, variations in the position or direction of the laser beam have no effect on the node positions, and as long as good stability is maintained between mirror and substrate, the periodicity of the pattern will be stable.

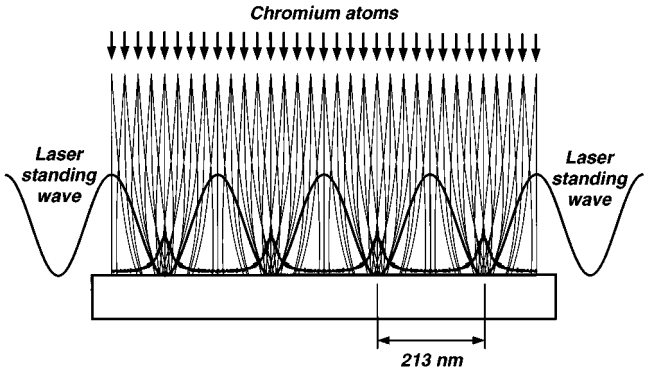

FIG. 1. One-dimensional schematic of laser-focused atomic deposition process, showing chromium atoms being focused by a laser standing wave into its nodes. The trajectories and the deposited peaks represent the results of actual calculations of the focusing process, though the relative vertical scales are highly distorted for clarity.

[a]Electronic mail: jabez@epg.nist.gov

For a two-dimensional deposition, the standing wave is formed by crossing two one-dimensional standing waves at 90° across the substrate. With this higher dimensionality, the nodes of the two-dimensional standing wave become more complex, depending on the polarizations of the constituent standing waves and also in some cases on their relative temporal phase. There are still zero points in the light intensity at locations on the surface that are an integral number of half-wavelengths from each standing wave mirror, but examination of an expression for the net electric field amplitude[7] shows that additional nodal patterns can exist, and these can shift around as the temporal phase difference between the standing waves varies.

One approach to eliminating unwanted variations in the nodal pattern due to temporal phase variations is to generate the two orthogonal standing waves in an actively-stabilized optical cavity.[8] Another approach,[9] which is useful when stability of the nodal topography is desired but absolute position is unimportant, makes use of three laser beams intersecting at 120°. For the present work we have made use of the fact that one can choose a polarization scheme in which the temporal phase does not affect the nodal pattern or position. If one chooses orthogonal linearly-polarized standing waves, with one polarized perpendicular to, and the other parallel to, the plane of the substrate, the resulting intensity distribution is given by

$$I(x,y)=4I_0(\sin^2 kx+\sin^2 ky) \tag{1}$$

where I_0 is the intensity of a single incident wave, $k=2\pi/\lambda$ is the wave vector of the light, and the x- and y-axes are defined to lie in the plane of the substrate. The intensity given by Eq. (1) forms a pattern of nodes and peaks on a $\lambda/2\times\lambda/2$ square lattice with the peaks separated by saddle regions along $\hat{\mathbf{x}}$ and $\hat{\mathbf{y}}$ at half the intensity.

While the intensity of Eq. (1) does not suffer from temporal phase disturbances, it has potential drawbacks that could in principle cause problems with a deposition experiment, though these appear to be less severe in practice. First, it might seem that since the intensity does not have cylindrical symmetry around the potential minima, the resulting deposited spots would not be round. However, the intensity is, in fact, surprisingly symmetric in the regions near the minima. This can be seen mathematically by converting x and y to the polar coordinates (r,θ) and noting that $I(r,\theta)\approx 4I_0k^2r^2$ (i.e., the θ-dependence drops out) for $kr\ll 1$. Exactly how much effect the non-symmetric regions of the potential (where kr is not much less than 1) have on the deposited pattern relative to the symmetric regions is difficult to predict without a ray-tracing calculation.[10] Nevertheless, the experimental results indicate that there is little effect.

Second, it must be noted that while the intensity in this configuration does not depend on the relative temporal phase, the polarization of the electromagnetic field is complicated. In fact, the local polarization varies dramatically as a function of x and y over the scale of a wavelength, and exactly what form this variation takes depends on the relative temporal phase. The local polarization of the field can be very important because it can determine the strength of the laser-atom interaction. Chromium atoms entering the standing-wave field are in their ground state, but are distributed among a number of degenerate magnetic sublevels. The strength of the laser-atom interaction for each magnetic sublevel varies for different polarizations of the laser, due to differences in the Clebsch-Gordan coefficients for the various transitions between the different magnetic sublevels.[11] The result is a potentially wide variation in the force on the atom as a function of space, and also time if the temporal phase is not stabilized.

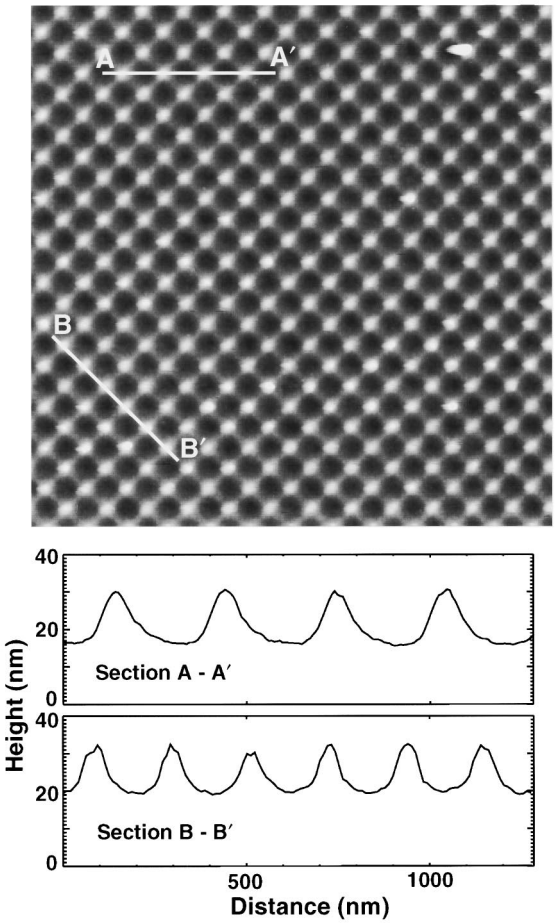

FIG. 2. Atomic force microscope (AFM) image of chromium features formed by laser-focused atomic deposition in a two-dimensional standing wave. The image covers a $4\mu\text{m}\times 4\mu\text{m}$ region of the sample. The features are on a square lattice with spacing 212.78 nm, which is determined by the laser wavelength. The standing wave is formed by superimposing two one-dimensional standing waves oriented at 45° and 135° to the figure. Also shown are two line scans, labeled A–A′ and B–B′, whose locations are indicated on the AFM image. The vertical scale for the line scans was determined by the AFM calibration, and the offset was estimated by requiring that the integral under the surface equal the total amount of material deposited, obtained from flux measurements.

Despite these potential problems, it appears that a sufficiently symmetric and stable potential exists for a well-defined pattern of features to be created. Figure 2 shows an atomic force microscope (AFM) image of a $4\ \mu\text{m}\times 4\ \mu\text{m}$ region of the two-dimensional chromium pattern deposited on a silicon substrate at room temperature. For this deposition, the laser beams for the two dimensions had $1/e^2$ diameters of 0.13 ± 0.02 mm and each contained a single-beam traveling-wave power of 12 ± 1 mW.[12] The total deposition

time was 20 min. The full pattern covers an area of about 100 μm$\times$200 μm, and is quite uniform across the entire area. The lattice constant of the pattern, $\lambda/2$ or 212.78 nm, was considered to be known more accurately than the horizontal calibration of the AFM, so this value was used to put the horizontal dimensions of the image on an absolute scale.

Also shown in Fig. 2 are two line scans, showing the shape of the features in two directions. These line scans have been put on a true vertical scale, including the background level, by normalizing the surface topography to the average deposition thickness of 20 nm, estimated (with an accuracy of about ± 5 nm) from previous characterizations of the deposition rate. Line scans such as the ones depicted in Fig. 2 and others taken at a variety of locations on the sample indicate that (without correction for AFM tip shape) the features are 13 ± 1 nm high, and have a full-width at half maximum of 80 ± 10 nm. The cause of the slight asymmetry in line scan A–A′ is unknown, though we believe it to be an AFM artifact.

As the line scans indicate, the regions between the features are also covered with chromium. This background is a result of other isotopes in the atomic beam which are not affected by the laser light (16% of the atoms), atoms which are transferred to the metastable D-state during the optical collimation step (an estimated 7% of the atoms), and atoms that are in the high velocity tail of the Maxwell-Boltzmann velocity distribution emerging from the chromium evaporation source. Scan B–B′ appears to have a slightly higher background level, arising we believe because it samples the saddle regions of the standing wave, while A–A′ samples the true nodes.

Various mechanisms could be implemented to reduce the background seen in Fig. 2, if desired. For example, the undesirable isotopes and D-level atoms, as well as some of the high velocity atoms, could be removed from the beam by a laser deflection process. Alternatively, it is possible that a uniform etch of the chromium surface as deposited could remove the background before eliminating the features completely.

This work demonstrates that laser-focused atomic deposition can be successfully used to create a uniform, two-dimensional nanometer-scale pattern on a substrate. In its current form, the pattern shown in Fig. 2 could prove extremely useful as a calibration standard on the nanometer scale. The features represent essentially a ''contact print'' of a light wave, the wavelength of which is tuned with extremely high precision to an atomic resonance whose frequency is know with very high accuracy (about 1 ppm). Thus, within the limits of some geometrical corrections that can be kept very small (of order 10 ppm or less), the lattice spacing accuracy is extremely high.

With additional enhancements of this technique, further applications can be envisioned. Elimination or removal of the background will result in the creation of an array of isolated nanoscale metal dots on a surface. These could be used to study, e.g., transport phenomena, or quantum dot effects if fabricated on a semiconductor. Further, they could be used as an etch mask[13] to transfer the pattern to a substrate material, allowing extension of the fabrication techniques to other materials. Improvement of the resolution, which should be possible down to the 10 nm level, could lead to the possibility of scanning the substrate during deposition, creating almost any desired pattern, replicated within each unit cell of the lattice across the substrate. Furthermore, the interference of many standing waves incident from a range of angles with controlled phase could be used to generate more complex patterns.

This work is supported in part by the Technology Administration of the U. S. Department of Commerce, and by the National Science Foundation under Grant no. PHY–9312572. Z. J. J. acknowledges support of a National Research Council postdoctoral fellowship.

[1] G. Timp, R. E. Behringer, D. M. Tennant, J. E. Cunningham, M. Prentiss, and K. K. Berggren, Phys. Rev. Lett. **69**, 1636 (1992).
[2] J. J. McClelland, R. E. Scholten, E. C. Palm, and R. J. Celotta, Science **262**, 877 (1993).
[3] R. E. Scholten, J. J. McClelland, E. C. Palm, A. Gavrin, and R. J. Celotta, J. Vac. Sci. Technol. B **12**, 1847 (1994).
[4] See, e.g., *Electron-beam, X-ray and Ion-beam Sub-micrometer Lithographies for Manufacturing II*, SPIE Proc. Vol. 1671, edited by M. Peckerar (SPIE, Bellingham, WA, 1992).
[5] R. E. Scholten, R. Gupta, J. J. McClelland, and R. J. Celotta (to be published).
[6] J. P. Gordon and A. Ashkin, Phys. Rev. A **21**, 1606 (1980); J. Dalibard and C. Cohen-Tannoudji, J. Opt. Soc. Am. B **2**, 1707 (1985).
[7] The net electric field can be determined by combining the four traveling waves $\mathbf{E}_{+x}=(\hat{\mathbf{z}}E_1+\hat{\mathbf{y}}E_2)e^{i(kx-\omega t)}$, $\mathbf{E}_{-x}=-(\hat{\mathbf{z}}E_1+\hat{\mathbf{y}}E_2)e^{-i(kx+\omega t)}$, $\mathbf{E}_{+y}=(\hat{\mathbf{x}}E_3+\hat{\mathbf{z}}E_4)e^{i(ky-\omega t+\phi)}$, $\mathbf{E}_{-y}=-(\hat{\mathbf{x}}E_3+\hat{\mathbf{z}}E_4)e^{-i(ky+\omega t-\phi)}$, where E_1 and E_2 are the complex electric field amplitudes determining the magnitude and polarization state of a wave traveling in the $+\hat{\mathbf{x}}$-direction, E_3 and E_4 are the corresponding amplitudes for a wave traveling in the $+\hat{\mathbf{y}}$-direction, and ϕ is the relative temporal phase for the two waves. See, e.g., J. D. Jackson, *Classical Electrodynamics*, 2nd ed. (Wiley, New York, 1975), pp. 273 ff.
[8] A. Hemmerich, D. Schropp, Jr., and T. W. Hänsch, Phys. Rev. A **44**, 1910 (1991).
[9] G. Grynberg, B. Lounis, P. Verkerk, J.-Y. Courtois, and C. Salomon, Phys. Rev. Lett. **70**, 2249 (1993).
[10] J. J. McClelland, J. Opt. Soc. Am. B (in press).
[11] For Cr, the variation can be as much as a factor of 28. See, e.g., V. G. Minogin and V. S. Letokhov, *Laser Light Pressure on Atoms* (Gordon and Breach, New York, 1987).
[12] Uncertainty estimates quoted in this paper are to be interpreted as one standard deviation combined random and systematic uncertainties unless otherwise indicated.
[13] N. I. Maluf, S. Y. Chou, J. P. McVittie, S. W. J. Kuan, . R. Allee, and R. F. W. Pease, J. Vac. Sci. Technol. B **7**, 1497 (1989).